ISSN: 2710-0170

Analysis of Running Ability for Coiled Tubing in Horizontal Wells

Ning Zhang, Hua Tong

School of Southwest Petroleum University, Chengdu 610000, China;

Abstract

Due to the large slenderness ratio and low bending stiffness of coiled tubing, it is prone to buckling and self-locking during operations in complex and long horizontal wells, thus failing to reach the target depth. To address this issue, a full-hole mechanical model for coiled tubing running is established in this paper, taking into account multiple factors including contact friction between coiled tubing and casing, fluid resistance inside and outside the tubing, and annular fluid lift force on the tubing. The influences of friction coefficient, residual initial stress and build-up rate on axial force, CT buckling and friction during running are investigated. The results show that a high friction coefficient increases the friction growth rate in the build-up section by 2–3 times and advances the tension-compression transition point by 430 m; a tensile residual stress of 50 MPa advances the neutral point by 131.7 m, while a compressive residual stress of −50 MPa delays compression by 156.57 m and reduces friction; a high build-up rate of 8°/30 m advances the neutral point by approximately 300 m and increases the peak friction by 90%.

Keywords

Coiled Tubing; Axial Load; Friction Coefficient; Build-up Rate.

1. Introduction

Compared with conventional tubing strings or ordinary drill strings, coiled tubing (CT) significantly reduces the complexity of downhole operations and enhances operational efficiency due to its continuity. Consequently, it has been widely applied in various stages of oil and gas exploration and production, including drilling, completion, logging, and workover operations[1]. However, as the current phase of oil and gas development progresses into the middle and late stages, production growth increasingly relies on extended-reach wells and horizontal wells, whose proportion has exceeded 65% of the total development in traditional oil and gas fields. Coiled tubing operations are no longer confined to a single mode of operation as in the past. When coiled tubing is deployed for downhole operations, the complex downhole environment may induce sinusoidal and helical buckling. This not only increases the difficulty of downhole operations but may also lead to operational accidents in severe cases. Therefore, research on the mechanical behavior of downhole coiled tubing is of great practical significance.

Over the years, scholars worldwide have conducted extensive and in-depth research on this topic, building upon existing theoretical foundations while considering complex boundary conditions and load variations. The most commonly employed research methods include analytical methods, energy methods, and finite element analysis. Mitchell[2] applied both the static equilibrium method and the energy method to investigate buckling behavior in constant-curvature wells, obtaining consistent conclusions regarding the sinusoidal critical load using both approaches. Chen[3] examined the influence of torque on the axial force transmission characteristics of CT in offshore "pipe-in-pipe" systems through theoretical analysis and experimentation. Zhuang Li[4] developed a set of partial differential equations incorporating the dynamic effects of coiled tubing (CT) based on the bending theory of slender beams under axial loading, yielding an analytical solution for sinusoidal deformation with time-dependent terms.

ISSN: 2710-0170

Jiewen Wang[5] established a comprehensive numerical framework to evaluate the fatigue performance of 4.5-inch CT. Tingting Qu[6] conducted various experimental analyses—including macroscopic observation, outer diameter and wall thickness measurements, physicochemical testing, magnetic particle inspection, Vickers hardness testing, optical microscopy, scanning electron microscopy, and energy dispersive spectroscopy—to investigate failed coiled tubing. Sokhoshko[7] developed a mathematical model for perforated horizontal gas wells with tubing positioned within the perforated interval, calculating gas inflow parameters, flow velocity along the wellbore, and fluid permeability in the bottomhole region. Wenlan Wei[8] constructed a CT-wellbore digital twin unit integrating the structure, physical fields, and materials of micro-element wellbore segments to enable dynamic identification and correction of contact states under various downhole trajectories. Zhuang Li[9] derived a set of partial differential equations incorporating dynamic effects of CT based on the bending theory of slender beams under axial loading, obtaining an analytical solution for sinusoidal deformation with time-dependent terms. Yingchun Chen[10] established an experimental "pipe-in-pipe" system test bench to simulate the effects of offshore loads and torque on CT. Dhrubajyoti Neog [11] analyzed the limitations of various CT grades (QT 800, QT 900, QT 1000) and established limit curves capable of describing operational boundaries and predicting CT failure probability.

In-depth investigations by domestic and international scholars on the mechanical analysis of coiled tubing (CT) have established a crucial theoretical foundation for understanding its buckling behavior. However, despite these research advancements, certain limitations persist in the study of CT buckling. Existing research often lacks a comprehensive consideration of the influencing factors. The buckling behavior of coiled tubing is affected by multiple factors, such as wellbore trajectory, drilling parameters, and the material properties of the CT[12]. Current studies tend to focus only on a subset of these factors, frequently neglecting the effects of friction coefficient, build-up rate, and initial residual stress. This leads to limitations in predicting and explaining CT buckling behavior, making it difficult to accurately and comprehensively reflect actual conditions. Moreover, most existing research remains concentrated at the theoretical level. This study investigates the mechanical behavior characteristics of coiled tubing under the specific wellbore trajectory of horizontal wells. By considering the contact friction between the CT and the casing, the internal and external fluid resistance, and the buoyancy force exerted by the annular fluid on the CT, a mechanical model for CT run-in-hole across the entire wellbore section is established. Theoretical calculations are performed to derive the axial force formula, and the distribution of axial force and friction under the influence of factors such as friction coefficient, build-up rate, and residual stress is thoroughly analyzed.

2. Analysis on Influencing Factors

2.1. Mechanical Model Establishment

Based on the micro-element method, the following fundamental assumptions are adopted when establishing the mechanical model for the entire wellbore of the coiled tubing: (1) The coiled tubing material is homogeneous and isotropic, conforming to Hooke's Law; (2) Only elastic deformation is considered, while plastic and geometric nonlinear effects are neglected; (3) The fluid flow is steady-state, and fluid forces are simplified as uniformly distributed or concentrated loads; (4) The wellbore is treated as a smooth curve, ignoring local irregularities.

Based on the forces acting on the coiled tubing in a horizontal well, an overall mechanical model of the coiled tubing during horizontal well operations is established, as shown in Figure 1. In the figure, L represents the vertical section, L1 represents the curved section, and L2 represents the horizontal section, where the radius of the curved section is r. T1, T2, and T3 denote the

ISSN: 2710-0170

axial forces acting on the coiled tubing in the vertical section, the build-up section, and the horizontal section, respectively. This paper will analyze the curved section and the horizontal section.

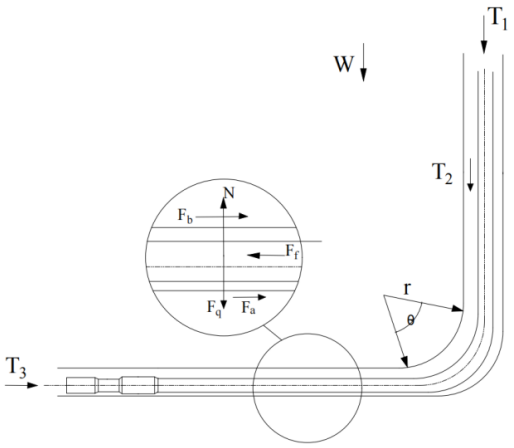

Fig. 1 Force Model of Coiled Tubing

A microelement is taken from the curved section, as shown in Fig 2.The microelement is subjected to the combined action of bending moment M, shear force, unit weight W, friction force, and tensile force.

The equilibrium equations are derived as follows:

$$\frac{dT_1(l)}{dl} = W\cos\theta - F_f \tag{1}$$

$$\frac{dQ(l)}{dl} = F_{N2} - W\sin\theta \tag{2}$$

$$dM - Q(l)dl + (F_{N2} - W\sin\theta)\frac{(dl)^2}{2} = 0 \tag{3}$$

According to the above formulas, the contact force must be calculated to determine the axial force. For the curved section, the contact force is given by:

$$F_{N2} = \frac{d^2M}{dL^2} - W\sin\theta \tag{4}$$

However, as the loads at both ends of the coiled tubing increase continuously, the initial equilibrium of the tubing string is broken and becomes unstable. When the load exceeds the critical load, sinusoidal buckling occurs in the coiled tubing. The critical load for sinusoidal buckling is given by:

$$F_{crs} = 2\sqrt{\frac{EIW\sin\theta}{r_c}} \tag{5}$$

Once sinusoidal buckling occurs in the coiled tubing, if the load further increases to another critical value, the buckling mode will transform into helical buckling. The formula for the critical load of helical buckling is given by:

$$F_{crh} = 2\left(2\sqrt{2}-1\right)\sqrt{\frac{EIW\sin\theta}{r_c}} \tag{6}$$

After buckling of the coiled tubing, an additional normal contact pressure will be generated, which requires correction of the contact force. The calculation formula is expressed as:

$$F_{NA} = \frac{cr_cT_e^2}{EI} \tag{7}$$

ISSN: 2710-0170

The contact force acting on the curved section is:

$$F_{NW} = F_{N2} + F_{NA} \tag{8}$$

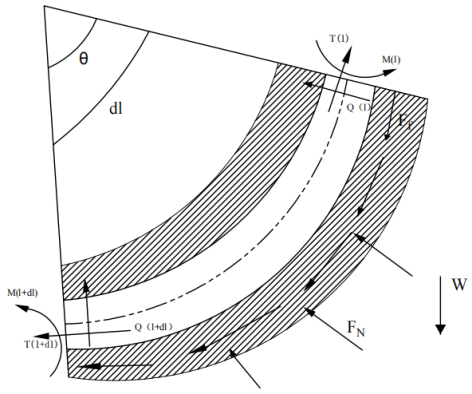

Fig. 2 curved section

A microelement of the horizontal section is selected as illustrated in Figure 3. Since the fluid flow is assumed to be steady-state, the fluid force is simplified as a uniformly distributed load. The uniformly distributed load includes: the buoyant weight of the coiled tubing and tool string, the contact force between the coiled tubing and the casing, the friction force between the coiled tubing and the casing, the friction force of the fluid inside the tubing, the friction force of the fluid outside the tubing, and the liquid lifting force exerted on the coiled tubing by the annulus.

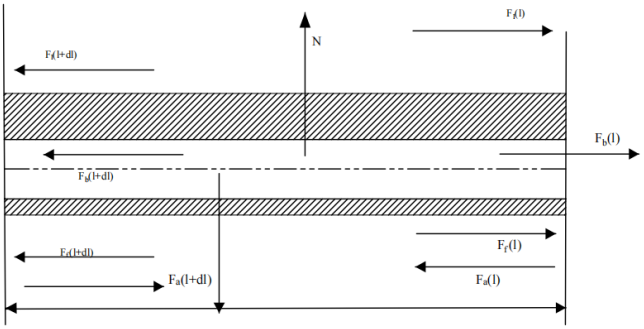

Fig. 3 horizontal section

Since the wellbore is usually filled with formation fluid, the tubing string is subjected to liquid buoyancy; therefore, the buoyant weight is adopted in the calculation and analysis. The buoyant weight per unit length of the tubing string is given by:

$$q_m = qK_f \tag{9}$$

The formula for the resistance per unit length is expressed as:

$$F_a = \frac{\pi}{2} f_i \rho_w (v_i - v_c)^2 D_i \tag{10}$$

Relative motion exists between the coiled tubing and the annulus fluid, which inevitably induces fluid frictional drag on the outer wall of the string. The frictional drag per unit length is:

$$F_b = -\frac{\pi}{2} D_o f_o \rho_w (v_a - v_c)^2 \tag{11}$$

When fluid flows inside and outside the string, the dynamic pressure generates a lifting force on the coiled tubing. The formula for the lifting force per unit length is:

$$F_1 = -\frac{2\pi D_o}{(D_a - D_o)} f_o \rho_w (v_a - v_c)^2 \tag{12}$$

ISSN: 2710-0170

Based on the above force conditions, the governing equation can be obtained as:

$$\frac{dT_2(L)}{dL} = F_b + F_f + F_1 - F_a \tag{13}$$

For the horizontal section, the contact force is equal to the buoyant weight of the tubing string.

To accurately analyze the mechanical behavior and deformation of coiled tubing in a three-dimensional wellbore, this study adopts the geometrically nonlinear beam element theory to establish a finite element model. For each element, the equilibrium equation is established in the local coordinate system, and then assembled into the structural equilibrium equation in the global coordinate system through coordinate transformation. By assembling the stiffness matrices and load vectors of all elements, the global equilibrium equation for analyzing the entire coiled tubing running into the horizontal well is constructed as:

$$[K]\{U\} = \{F\} \tag{14}$$

2.2. boundary conditions

The boundary conditions at the wellhead are set as follows: lateral displacements are $u_x = u_\gamma = 0$; axial displacement is $u_2 = 0$; the force is $F_2 = F_0$; bending moments are $M_x = M_\gamma = 0$. The build-up rate for the curved section is 8°/30m. The inclination angle of the horizontal section is 88°. The casing inner diameter is 74.44 mm. The preliminary dimensions selected for the coiled tubing are: outer diameter D_0 = 50.8 mm, inner diameter D_i = 42.5 mm, and wall thickness t = 3.2 mm. The linear weight of the pipe string is 40.24 N/m, the elastic modulus is 203 GPa, Poisson's ratio v = 0.3, density ρ = 7850 kg/m^3, yield strength σ_γ = 400 MPa, and the friction coefficient in the cased hole section is μ = 0.25. The friction coefficient in the open hole section is μ = 0.38.

Based on measured data from a specific well, the coiled tubing trajectory parameters were obtained and a fitted curve was generated. The coiled tubing is divided into three sections: the vertical section, the build-up section, and the horizontal section.

The three-dimensional wellbore trajectory is shown in Figure 4. The vertical section: the drill rate is constant in the vertical section, with the surface coordinates anchored at (0,0,0), establishing an absolute spatial reference. The build-up section: a critical zone for directional vector change, achieving an 88° inclination angle with a build-up rate of 5°/30m. The horizontal section: extends steadily at a constant angle. Based on this trajectory, the wellbore trajectory parameter table, Table 1, is generated.

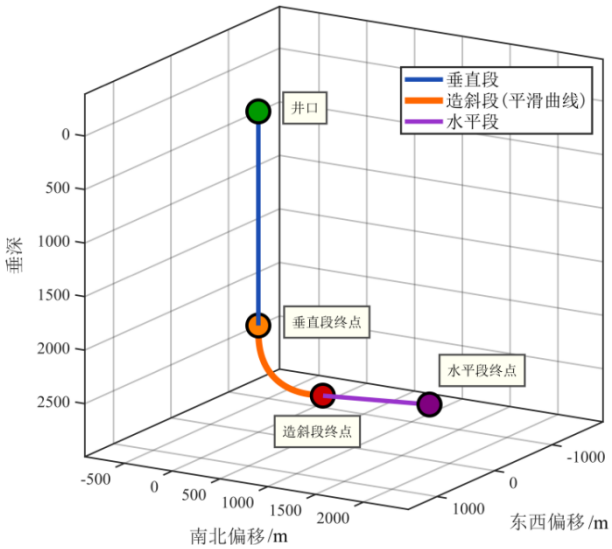

Fig. 4 3D wellbore trajectory

ISSN: 2710-0170

Table 1 Wellbore Trajectory Parameter Table

Measured Depth/m	Interval Length/m	Dogleg Severity/(°/30m)	True Vertical Depth/m	Remark
0	0	0	0	Wellhead
2000	2000	0	2000	End of Vertical Section
2500	500	4.5	2500	End of Build-up Section
4000	1500	0	2500	End of Horizontal Section

The running of coiled tubing is a process involving multiple factors, and its operational effectiveness directly impacts the safety and economy of downhole operations. Research on the mechanical properties of coiled tubing is based on elastic-plastic mechanics and the buckling theory of slender rods[13]. During the running process, the tubing is subjected to the combined effects of axial compression, bending stress, and torsional stress.

The mechanical properties of the coiled tubing itself are key factors determining its runnability. Parameters such as the tubing material, diameter, wall thickness, yield strength, and residual stress collectively influence the stiffness, buckling resistance, and fatigue life of the coiled tubing within the wellbore[14]. In the build-up or horizontal sections, increased contact force between the tubing and the wellbore may lead to lock-up or helical buckling. The critical load for this is directly related to the tubing's geometric dimensions and material mechanical characteristics[15]. External factors such as wellbore trajectory and borehole conditions also affect the running of coiled tubing. Variations in borehole diameter, dogleg severity, wellbore roughness, and the presence of underreaming all influence the contact state and frictional resistance between the tubing and the wellbore. More complex three-dimensional wellbore trajectories result in associated bending stresses and axial frictional forces[16], further affecting the efficiency of transmitting effective thrust to the bottom hole.

In addition to the factors mentioned above, the density, rheology, and lubricity of the drilling fluid or completion fluid in the annulus are also important. These factors determine the circulating pressure drop, suspension and cuttings transport capacity, and the friction coefficient. This chapter does not consider dynamic factors and selects three factors—friction coefficient, residual initial stress, and build-up rate—to investigate the running of coiled tubing.

2.3. Analysis of Influencing Factors

2.3.1. Influence of Friction Coefficient on Coiled Tubing Run-In-Hole Process

The variation patterns of axial force and frictional resistance for coiled tubing in a horizontal well were calculated under three different friction coefficient conditions (μ=0.12, μ=0.25, and μ=0.38), as shown in Figure 5. The figure illustrates that within the 0-2000m interval, when the friction coefficient is 0.12, the axial force decreases from 85 KN to 10.18 KN, a reduction of 88.02%; when the friction coefficient is 0.25, the axial force decreases from 105 KN to 6.21 KN, a reduction of 94.9%; and when the friction coefficient is 0.38, the axial force decreases from 125 KN to 1.13 KN, a reduction of 99.10%. Based on these values, a phenomenon of rapid axial force decline can be clearly observed. The fundamental reason for this lies in the coupling effect between the self-weight of the coiled tubing and frictional resistance.

In the vertical well section, the string's self-weight is the dominant factor in the reduction of axial force. However, upon entering the build-up section, the increase in inclination angle leads to a rise in the normal contact force between the string and the wellbore. Consequently, the curves begin to diverge significantly, with the axial force down being more pronounced under high friction coefficient conditions. When the axial force decreases to a negative value, it indicates that the coiled tubing has transitioned from a state of tension to one of compression: as the running depth increases, the accumulated frictional resistance gradually exceeds the

ISSN: 2710-0170

effective thrust transmitted from the surface, resulting in axial compressive force at the bottom end of the string. Regarding the position of the neutral point under different friction coefficients: the larger the friction coefficient, the earlier the neutral point occurs.

The trend of axial force recovery observed in the deep horizontal section is primarily attributed to changes in the geometric characteristics of the wellbore trajectory. Upon entering the horizontal section, the inclination angle stabilizes, causing the contact mode between the string and the wellbore to transition from line contact to relatively gentle surface contact. This reduces the growth rate of frictional resistance per unit length. Simultaneously, in the horizontal section, the contribution of the string's self-weight to axial force is converted into lateral support force, no longer directly consuming axial thrust. This change in geometric effects leads to an upward trend in axial force.

A study on the axial force at 4000m is presented in Table 2.

Table 2 Axial force at 4000 m

Friction Coefficient	0.12	0.25	0.38
Axial Load (KN)	-14.57	-7.89	0.00

According to this table, when the friction coefficient is 0.12, the corresponding axial force is -14.57 KN; when the friction coefficient is 0.25, the corresponding axial force is -7.89 KN. This indicates that a sufficient axial compressive load still acts on the front end of the pipe string, allowing continued running. When the friction coefficient is 0.38, the corresponding axial force is 0 KN, indicating that the thrust transmission capacity has reached its upper limit and further running is impossible.

Figure 5 illustrates the variation in frictional drag distribution along the horizontal wellbore for coiled tubing under different coefficients of friction ($\mu = 0.12$, $\mu = 0.25$, and $\mu = 0.38$). During the entire run-in-hole process of the coiled tubing, the frictional drag consistently increases with measured depth, and the coefficient of friction significantly influences the rate of this increase. In the shallow section (0-1000 m), the frictional drag remains relatively low, primarily due to the small inclination angle and limited contact force, which results in an insignificant frictional effect. As the well depth increases and the tubing enters the build-up section, the inclination angle gradually rises. This leads to a sharp increase in the normal contact force between the tubing string and the wellbore wall, causing a distinct divergence in the frictional drag curves. Under the high friction coefficient condition ($\mu = 0.38$), the curve exhibits the steepest slope, indicating the most rapid increase in frictional drag. Conversely, under the low friction coefficient condition ($\mu = 0.12$), the frictional drag increases at a relatively gentler rate. In the deep horizontal section, where the inclination angle stabilizes at 90° and the radius of curvature increases, the incremental frictional drag per unit length diminishes, and the frictional drag curves tend to stabilize.

The variation in the friction coefficient essentially reflects the combined effects of the tubing surface characteristics, wellbore conditions, and lubricity. A high friction coefficient not only results in elevated overall frictional drag throughout the entire wellbore but also potentially reduces running efficiency and increases operational risks. Understanding this behavior provides a theoretical basis for frictional drag control and the optimization of operational parameters during the horizontal run-in-hole of coiled tubing.

2.3.2. Operations

Set three residual initial stress conditions: σ_{res} = -50 MPa, 0 MPa, and 50 MPa. A positive residual initial stress primarily induces tension in the coiled tubing, while a negative residual initial stress primarily induces compression. An investigation was conducted to analyze the influence of different residual initial stresses on the running process of coiled tubing in horizontal wells.

ISSN: 2710-0170

As illustrated in Figure 6, the analysis of the axial force distribution and running depth reveals the following: In the vertical well section, under the condition of positive residual stress, a greater control force is required at the surface to maintain the overall state at the same depth. Conversely, for negative residual stress, the effective pulling force needed at the wellhead is slightly lower. The work with positive residual stress exhibits the fastest rate of axial force down, whereas the work with negative residual stress shows the slowest down rate.

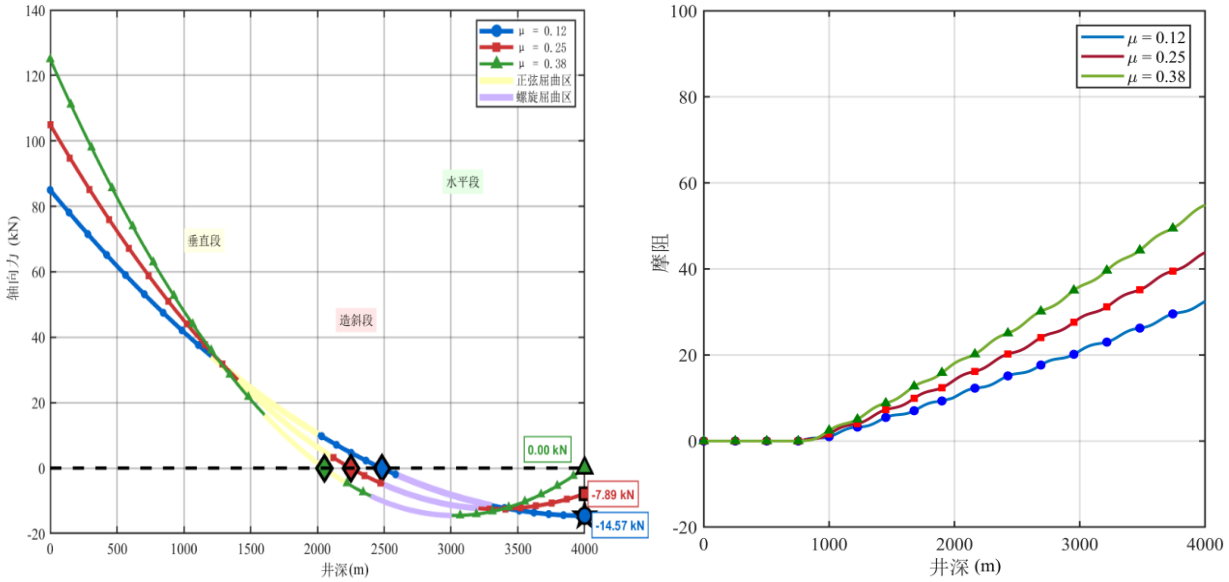

Fig. 5 Effect of different friction coefficients on axial force and friction drag of coiled tubing

2.3.3. Effect of Different Residual Initial Stresses on Coiled Tubing Run-In-Hole The neutral point depth corresponding to each condition, along with the attainable maximum running depth, is presented in Table 3.

Table 3 corresponding neutral point depth, and maximum reachable depth

Initial residual stress (MPa)	-50	0	50
Corresponding neutral point depth (m)	2353.54	2196.97	2065.27
Maximum reachable depth (m)	4000.00+	4000.00	3610.4

As the coiled tubing enters the build-up section, under the σ_{res}=50 MPa condition, the neutral point (where axial force transitions from tension to zero) shifts upward due to the tensile residual stress. Under the σ_{res}=0 MPa condition, the tension is sustained to a greater depth before transitioning into compression. In contrast, under the σ_{res}=-50 MPa condition, partial cancellation of the bending-induced tensile stress results in the shallowest neutral point depth.

Upon entering the horizontal section, the influence of residual stress on axial force distribution becomes more pronounced. The axial force curve under the σ_{res}=50 MPa condition exhibits a steeper upward trend, leading to earlier onset of yielding, with a maximum running depth of 3610.4 m. The σ_{res}=0 MPa condition represents an intermediate case, achieving a running depth of 4000.0 m, which is 10.79% greater than that of the σ_{res}=50 MPa condition. Under the σ_{res}=-50 MPa condition, partial offset of tensile stress results in a relatively gradual upward trend, delaying yielding and preserving downward force transmission at 4000 m, thereby enabling a greater running depth.

The following conclusions can be drawn: Under identical wellbore conditions, negative residual stress yields the optimal mechanical performance and the greatest running depth, followed by zero residual stress. Positive residual stress is the most unfavorable, significantly compromising safety performance and maximum running depth.

ISSN: 2710-0170

Residual initial stress does not directly influence frictional resistance; rather, it affects frictional distribution by altering the normal force between the tubing and wellbore and by inducing tubing buckling. As illustrated in Figure 6, the effect of residual initial stress on frictional resistance is analyzed as follows: In the vertical section, the coiled tubing hangs under its own weight with minimal contact force against the wellbore, resulting in negligible frictional resistance. Upon entering the build-up section, the curves begin to diverge. Compressive residual stress reduces the effective pushing force, rendering the tubing more compliant and leading to tighter contact with the wellbore in curved intervals, thereby causing a slight increase in contact force. Tensile residual stress, by contrast, enhances the effective pushing force and partially mitigates excessive contact with the wellbore. In the horizontal section, the disparity in frictional resistance becomes most pronounced, with maximum sensitivity to residual stress. Under the σ_{res}=50 MPa condition, tensile residual stress partially offsets the operational compressive load, helping the tubing maintain a straightened configuration in the horizontal section. Contact is primarily confined to natural sag contact with the low side of the wellbore, resulting in minimal contact force and the lowest frictional resistance. Under the σ_{res}=0 MPa condition, frictional resistance remains relatively stable at an elevated level, as the tubing contacts the low side of the wellbore under its own weight, generating steady contact force. Under the σ_{res}=-50 MPa condition, the tubing is highly susceptible to buckling under compressive loading, leading to multiple contact points or even full engagement with the wellbore wall. This results in the highest frictional resistance and stepwise increases, which fundamentally limits running depth under compressive residual stress.

The presence of residual stress modifies the actual downhole stress state experienced by the tubing, introducing deviations from theoretical calculations based solely on external loads. Under axial compressive loading, residual stress may prematurely induce yielding or plastic deformation, reducing the tubing's collapse resistance and fatigue life. Interactions between residual stress and gravitational distribution may cause geometric changes in the tubing, increasing contact friction with the wellbore, thereby impairing axial force transmission efficiency and leading to inaccuracies in predicting ultimate running depth. Therefore, quantifying residual initial stress is of significant value for enhancing the safety and reliability of running operation design.

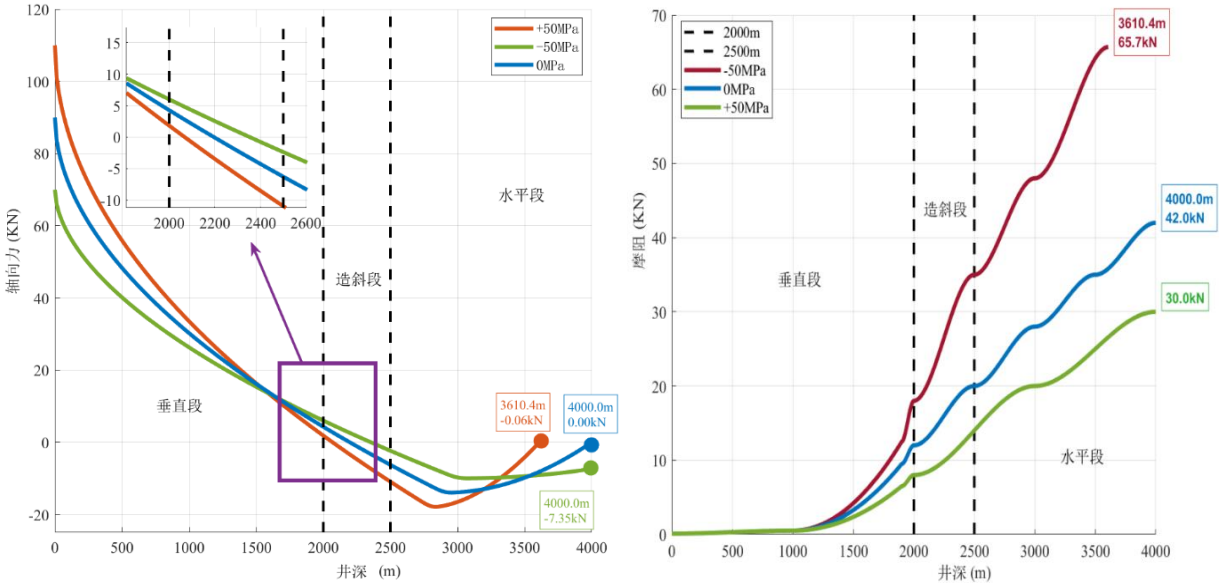

Fig. 6 Effect of different initial residual stresses on axial force and friction drag of coiled tubing

2.3.4. Impact of Different Build-Up Rates on Coiled Tubing Run-In-Hole Performance

The build-up rate is one of the core factors affecting coiled tubing run-in-hole. When coiled tubing passes through the build-up section, it must bend to conform to the wellbore trajectory.

ISSN: 2710-0170

The bent tubing will press against the outer side of the wellbore, generating a normal contact force that is proportional to the build-up rate. Analyzing the impact of the build-up rate on coiled tubing run-in-hole, the distribution of axial force under three build-up rate conditions (low: 2°/30m, medium: 4°/30m, and high: 8°/30m) is presented in Figure 7. At the wellhead position, it can be observed that the wellbore scenario with a build-up rate of 2°/30m exhibits the smallest axial force, while the scenario with a build-up rate of 8°/30m exhibits the largest axial force. This is because a higher build-up rate results in greater cumulative frictional drag, thus requiring a larger pushing force at the wellhead. In the vertical section, all three curves show a downward trend. The higher the build-up rate, the greater the magnitude of the axial force decrease, and concurrently, the position of the neutral point advances further with an increasing build-up rate. In the build-up section, the substantial bending-induced normal pressure generates an upward frictional resistance, which significantly consumes the pushing force transmitted from above, causing a sharp decline in all three curves. For a high build-up rate in a short, sharp curved section, the axial force exhibits a very steep drop, whereas for a low build-up rate in a long, gradual curved section, the axial force decrease is relatively gentle. The depth corresponding to the neutral point and the axial force at 4000m are shown in Table 4.

Table 4 Corresponding neutral point depth and axial force at 4000 m

Build-up rate	2°/30m	4°/30m	8°/30m
Corresponding neutral point depth (m)	2395.47	2245.61	2095.24
Axial force at 4000 m (KN)	-9.34	-1.43	0.00

Based on the data in this table, it is observed that a higher build-up rate leads to an earlier occurrence of the neutral point. Specifically, at a build-up rate of 2°/30m, the neutral point is located at 2395.47m; whereas at a build-up rate of 8°/30m, it advances to 2095.24m, representing a relative shift of 12.53%. Regarding the axial force at the depth of 4000m, at a build-up rate of 2°/30m, the axial force is -9.34 KN. At a build-up rate of 4°/30m, it is -1.43 KN, indicating that the front end of the coiled tubing still retains some downward force. However, at a build-up rate of 8°/30m, the axial force reduces to 0 KN, signifying that the maximum run-in-depth has been reached. This phenomenon occurs because a high build-up rate dissipates excessive energy in the build-up section. Consequently, the axial force remaining upon reaching the start of the horizontal section is minimal. In contrast, a lower build-up rate preserves a certain amount of axial force at the entry point of the horizontal section, allowing for deeper penetration.

Therefore, a gradual build-up section significantly enhances the efficiency of axial force transfer and is the most critical factor for ensuring the successful run-in-hole of coiled tubing to the target depth.

Analyzing the influence of the build-up rate on frictional drag during coiled tubing run-in-hole, the distribution of frictional drag under three build-up rate conditions (low: 2°/30m, medium: 4°/30m, and high: 8°/30m) is presented in Figure 7. In the vertical section, the weight of the coiled tubing hangs directly within the wellbore, resulting in very minimal contact force with the wellbore wall and, consequently, negligible frictional drag. As run-in-hole continues into the build-up section, the coiled tubing must overcome not only the frictional drag generated by its weight but also the substantial additional positive pressure induced by the wellbore curvature. Frictional drag begins to accelerate, with the curve's slope steepening noticeably. This inflection point becomes more pronounced, and the slope steeper, with higher build-up rates. As the inclination angle increases, the radial component of the gravitational force begins to contribute to the positive pressure as well. This radial force superimposes onto the positive pressure generated by the curvature, causing a sharp rise in frictional drag. In high build-up rate sections, sinusoidal or helical buckling is highly likely to be triggered, at which point

ISSN: 2710-0170

frictional drag becomes extremely large. When helical buckling develops to a certain degree, the pushing force intended to advance the coiled tubing is entirely consumed by the enormous frictional drag, preventing force transmission and leading to an inability to run further-a phenomenon known as “lock-up”. Upon entering the horizontal section, the wellbore trajectory transitions from build-up to hold. No new curvature-induced positive pressure is generated. Here, the positive pressure is primarily produced by the weight of the tubing in its horizontal configuration. Consequently, the rate of increase in frictional drag abruptly slows, the curve's slope flattens, though drag continues to accumulate.

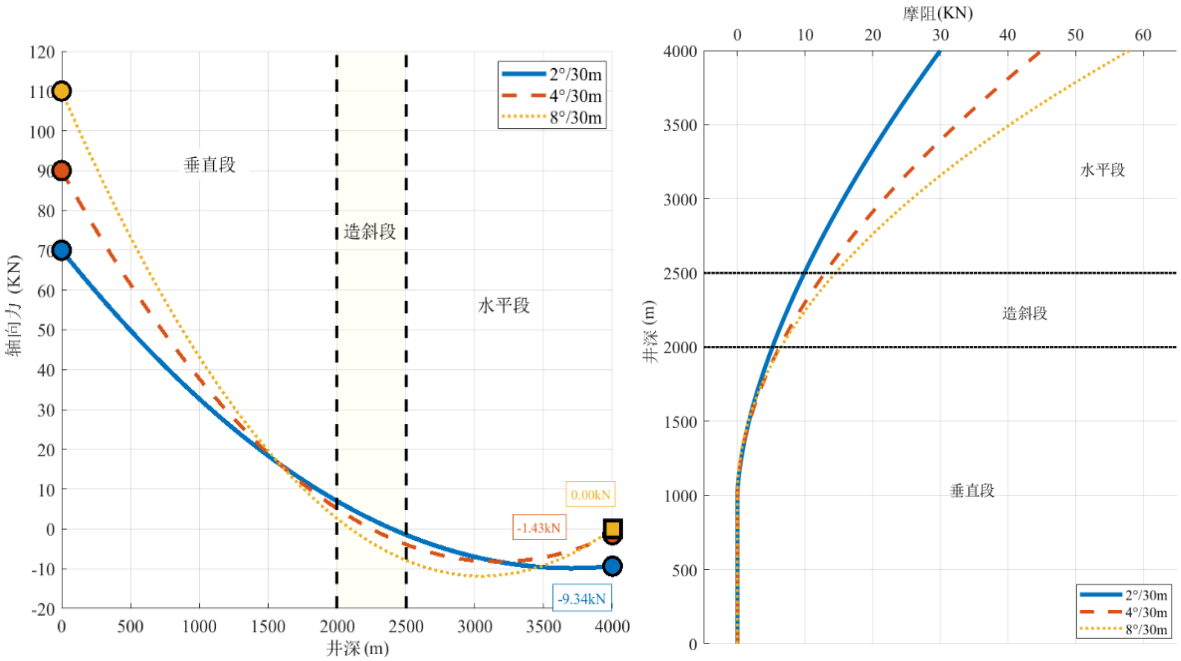

Fig. 7 Axial force and friction drag distribution under different build-up rates

The investigation into the effects of wellbore trajectory on axial force and frictional drag during coiled tubing run-in-hole indicates that a high build-up rate is the dominant factor causing a dramatic increase in frictional drag. This is primarily because the build-up rate directly dictates the degree of tubing bending and the resulting contact force against the wellbore wall. This, in turn, nonlinearly amplifies the sliding frictional drag according to Coulomb's friction law. This effect is particularly pronounced in the build-up section, where substantial axial force can be consumed. This consumption leads to an upward shift of the neutral point, compression in the lower tubing string, and the risk of lock-up. The variation in frictional drag across the entire wellbore exhibits segmented characteristics: it accumulates linearly in the vertical section; the build-up section generates the core frictional drag increment due to geometric constraints; and the horizontal section presents further complexity due to sustained positive pressure and potential helical buckling effects.

Consequently, effective frictional drag control necessitates the comprehensive optimization of the build-up section design to balance local bending intensity against the total frictional path. It is also crucial to strictly prevent the vicious cycle of buckling, which can be triggered by excessive axial compression.

3. Summary

The contact friction between coiled tubing and casing, the resistance from internal and external fluids, and the lifting force exerted by the annular fluid on the coiled tubing were considered to establish a mechanical model for the entire wellbore during coiled tubing run-in-hole operations. This model fully accounts for influencing factors such as friction coefficient, build-

ISSN: 2710-0170

up rate, and residual stress in analyzing axial force and friction distribution. The following conclusions can be drawn:

(1) During the run-in-hole process of coiled tubing in horizontal wells, the influence of the friction coefficient on axial force and friction was analyzed. The results indicate that friction increases monotonically along the well depth, with the growth rate of friction in the build-up section being significantly faster than in other sections. Under high friction coefficient conditions, the slope of the friction curve is two to three times that under low friction coefficient conditions. The axial force transitions from tension to compression in the build-up section, with the transition point occurring earlier as the friction coefficient increases. For μ=0.38, the transition point is 430 m earlier compared to μ=0.12. A high friction coefficient exacerbates the risk of axial compressive force approaching the critical buckling load. Upon entering the horizontal section, the friction curve tends to stabilize but remains at a high level.

(2) The influence of different residual stresses on the axial force and friction distribution of coiled tubing during run-in-hole operations in horizontal wells was studied. The research shows that tensile residual stress (σ_{res}=50 MPa) advances the transition to the compression state by 131.7 m, resulting in a maximum friction force 19% higher than under compressive conditions. This significantly increases the likelihood of buckling, thereby limiting the run-in-hole depth. Compressive residual stress (σ_{res}=−50 MPa), on the other hand, delays the transition point to compression by 156.57 m, resulting in a smaller maximum friction force compared to other conditions. Therefore, appropriate compressive residual stress can enhance operational efficiency and structural stability.

(3) The impact of build-up rate on axial load calculation for coiled tubing was analyzed: the higher the build-up rate, the faster the axial force decays in the build-up section and the steeper the friction increases. For a high build-up rate (8°/30 m), the neutral point occurs approximately 300 m earlier than for a low build-up rate, with the peak friction force being about 90% higher. This increases the risk of inducing helical buckling or even lock-up. A low build-up rate (2°/30 m) improves force transmission efficiency, reduces friction, and extends the run-in-hole depth.

References

[1] Liangjie MaoCA,Yuan Yuan,Jiefei Luo,et al. Feasibility analysis of coiled tubing running into long horizontal wells of shale gas[J]. Petroleum Science and Technology,2025,: 1-25.

[2] Mitchell, R.F.. Simple Frictional Analysis of Helical Buckling of Tubing[J]. SPE Drilling Engineering,1986,Vol.1(6): 457-465.

[3] Chen, Yingchun,Li,et al. Axial force transfer characteristics of a coiled tubing conducting offshore rotary operation.[J]. Ocean Engineering,2021,Vol.242: 110112.

[4] Zhuang Li ,Liangyu Chen,Fei Yuan & …Lei Zhao. Study on helical post-buckling of motional coiled tubing in horizontal wells[J]. Journal of Petroleum Exploration and Production Technology, 2025, Vol.15(6): 1-18.

[5] Jiewen Wang,Ziye Wang,Lei Gao,et al. Fatigue analysis and life prediction of 4.5-inch UDRIS coiled tubing[J]. Results in Engineering,2025,Vol.28: 107987.

[6] Ting-ting QuCA1,Ke Tong,Hong Li,et al. Investigation and analysis of fracture failure of TS-110 coiled tubing used in oil and gas field in southwest China[J]. Engineering Failure Analysis, 2023,Vol.147: 107153.

[7] Sokhoshko, S. K..Modeling and designing the features of inflow to a horizontal gas borehole fitted with coiled tubing within the filtering interval[J]. BULLETIN OF THE TOMSK POLYTECHNIC UNIVERSITY-GEO ASSETS ENGINEERING,2024,Vol.335(1): 194-201.

[8] Wenlan WeiCA,Hao Qu,Jiarui Cheng,et al. Digital twin and contact analysis of ultra-long distance coiled tubing operation structures[J]. Digital Twin,2025,Vol.2(3): 2530305.

ISSN: 2710-0170

[9] Zhuang Li,Liangyu Chen,Yan Zhong,et al. Study on Sinusoidal Post-Buckling Deformation of Coiled Tubing in Horizontal Wells Based on the Separation Constant Method[J]. Machines,2023,Vol.11(5): 563.

[10] Yingchun ChenCA1,Yanfeng Li. Study on axial force characteristics of coiled tubing rotating operation in marine riser under helical post-buckling[J]. Ocean Engineering,2022,Vol.261: 112098.

[11] Dhrubajyoti NeogCA1,Ankur Sarmah,Mohammad Irfan Sunny Baruah. Computational analysis of coiled tubing concerns during oil well intervention in the upper Assam basin, India[J]. Scientific Reports,2023,Vol.13(1): 1795.

[12] Zhang, Jiantao, Yin,et al. The helical buckling and extended reach limit of coiled tubing with initial bending curvature in horizontal wellbores[J]. Journal of Petroleum Science and Engineering, 2021,Vol.200: 108398.

[13] Christopher Bridge,Andrew C. Palmer,Simon Falser. Interaction between a compliant guide and a coiled tubing during sub-sea well intervention in deep water[J]. Applied Ocean Research, 2010,Vol.32(4): 454-459.

[14] Antonio Contreras Cuevas,Lucila Cruz-Castro,Apolinar Albiter HernándezCA1. Failure analysis due to collapse pressure in CT-90 coiled tubing in the Mexican oil industry[J]. Journal of Pipeline Science and Engineering,2026,Vol.6(1): 100303.

[15] Li Yanfeng, Chen Yingchun.Analysis of axial force transmission characteristics and contact mechanism of coiled tubing in the spoolable compliant guide during injection[J]. Ocean Engineering. 2023.

[16] Zhang Jiantao, Yuan Liang, Yan Hanbing.Helical buckling of coiled tubing with initial bending curvature in three-dimensional curved wellbores[J]. Geoenergy Science and Engineering.2024.